SUPPLEMENTAL MATERIAL

# Exploiting multi-wavelength aerosol absorption coefficients in a multi-time source apportionment study to retrieve source-dependent absorption parameters

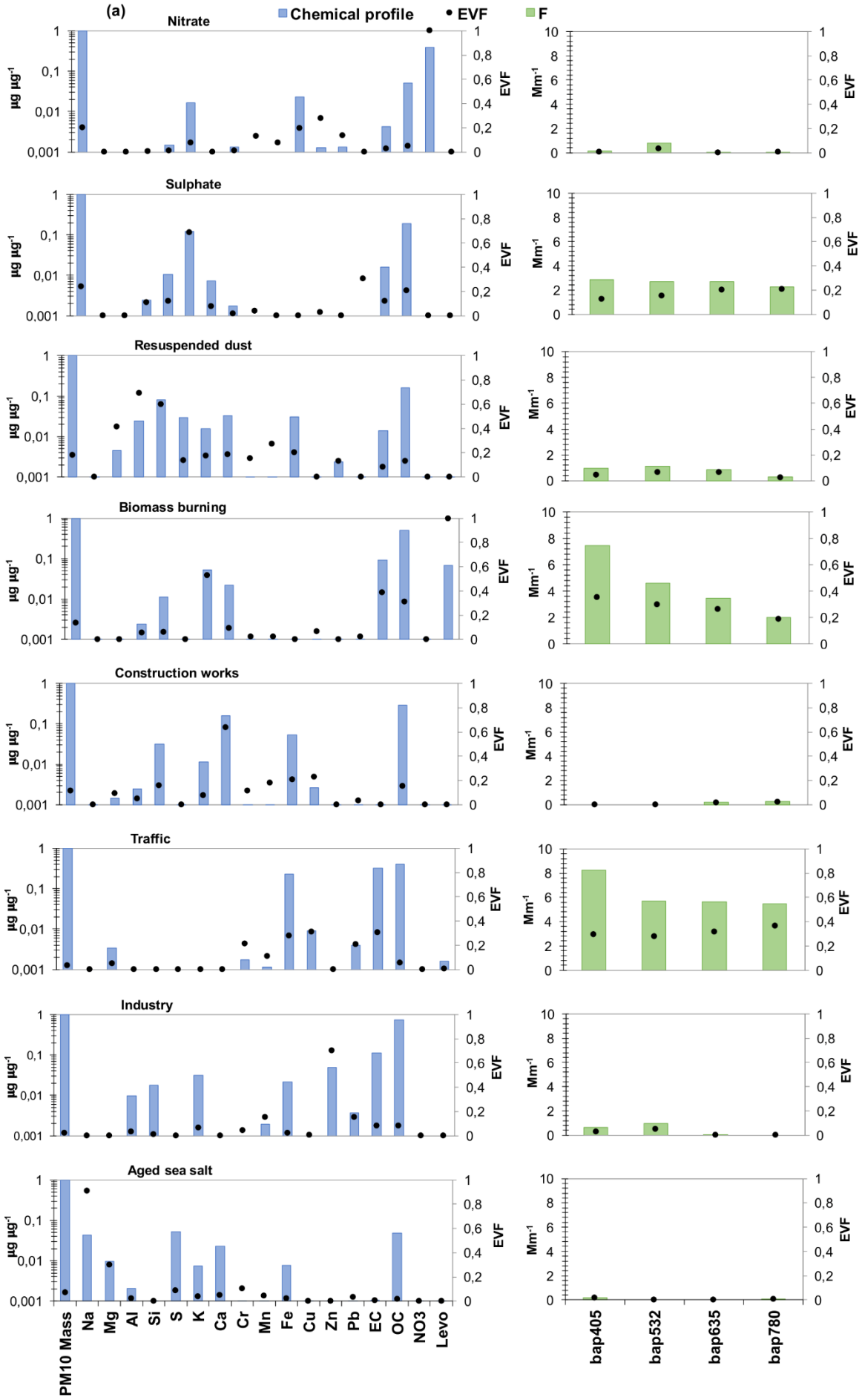


Figure S1: (a) Chemical profiles of the 8-factor base case solution (b) $b_{ap}$ apportionment of the 8-factor base case solution.

| Factors | Total [$\mu$g m$^{-3}$] |
|---|---|
| Nitrate | 10.4 (31 %) |
| Sulphate | 6.2 (19 %) |
| Resuspended dust | 5.5 (16 %) |
| Biomass burning | 3.5 (11 %) |
| Construction works | 3.6 (11 %) |
| Traffic | 1.7 (5 %) |
| Industry | 1.1 (3 %) |
| Aged sea salt | 1.3 (4 %) |

Table S1: Absolute and relative average source contributions to PM10 mass in the 8-factor base case solution.

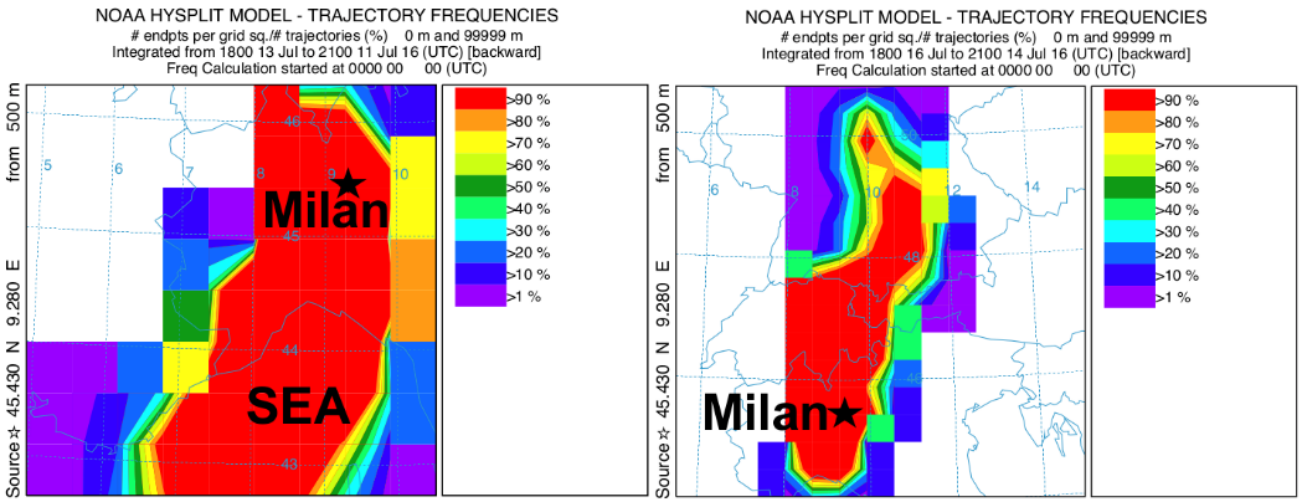


Figure S2: On the left, frequencies before and during the sea salt transport event; on the right, frequencies after the sea salt transport event.

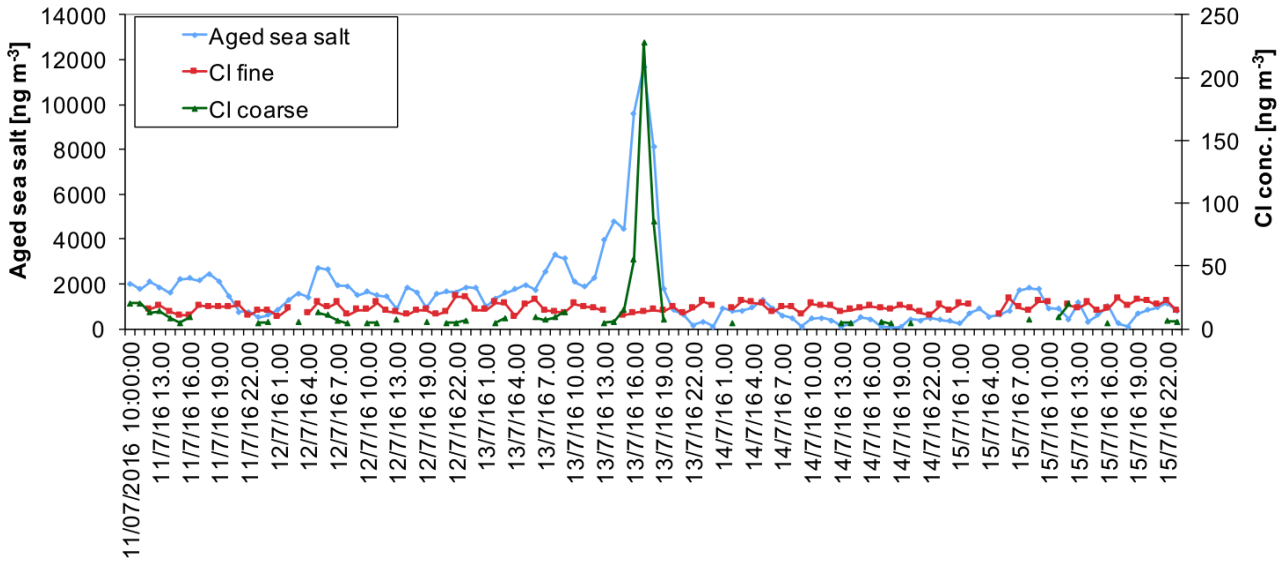


Figure S3: Temporal patterns of aged sea salt source retrieved from the multi-time model and Cl concentrations measured in atmosphere in the fine and coarse fractions.

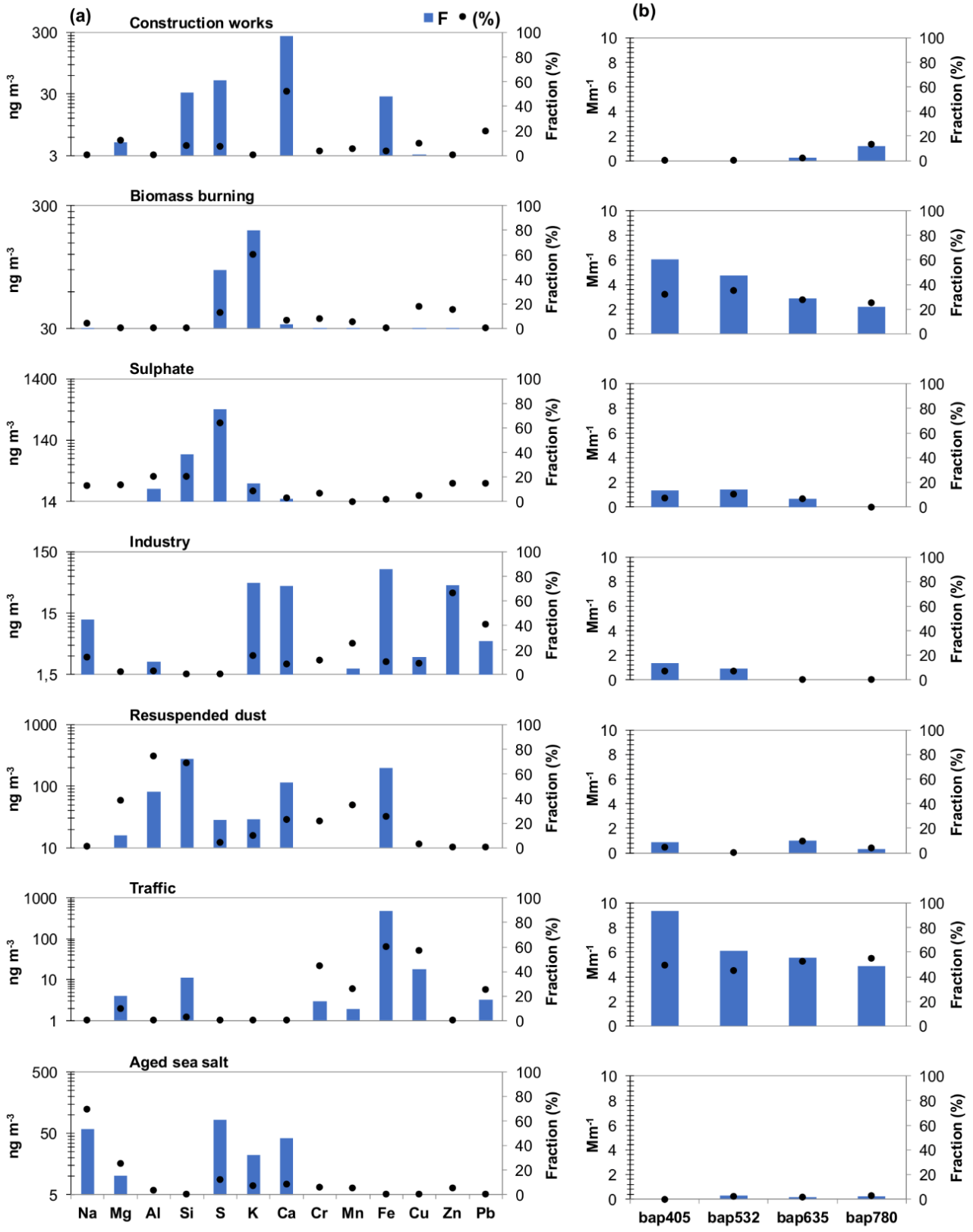


Figure S4: Source apportionment study performed with EPA PMF 5.0 on elemental concentrations and absorption coefficients at four wavelengths, both measured on high-time resolution samples collected by streaker sampler.

| *Measured in atmosphere* | **$\lambda$ = 405 nm** | | | **$\lambda$ = 532 nm** | | | **$\lambda$ = 635 nm** | | | **$\lambda$ = 780 nm** | | |
|---|---|---|---|---|---|---|---|---|---|---|---|---|
| | ***$b_{ap}$/EC*** | ***$\sigma$*** | ***$R^2$*** | ***$b_{ap}$/EC*** | ***$\sigma$*** | ***$R^2$*** | ***$b_{ap}$/EC*** | ***$\sigma$*** | ***$R^2$*** | ***$b_{ap}$/EC*** | ***$\sigma$*** | ***$R^2$*** |
| **Summer** | **14.2** | ± 0.5 | 0.61 | **12.9** | ± 0.5 | 0.61 | **11.1** | ± 0.4 | 0.64 | **9.8** | ± 0.4 | 0.67 |
| **Winter** | **17.8** | ± 0.4 | 0.89 | **12.8** | ± 0.3 | 0.90 | **11.2** | ± 0.3 | 0.87 | **8.9** | ± 0.3 | 0.79 |
| **All data** | **17.3** | ± 0.3 | 0.94 | **12.8** | ± 0.2 | 0.94 | **11.2** | ± 0.2 | 0.93 | **9.0** | ± 0.2 | 0.87 |
| ***Multi-time model*** | **$b_{ap}$/EC** | **$25^{th}$-$75^{th}$ percentile** | | **$b_{ap}$/EC** | **$25^{th}$-$75^{th}$ percentile** | | **$b_{ap}$/EC** | **$25^{th}$-$75^{th}$ percentile** | | **$b_{ap}$/EC** | **$25^{th}$-$75^{th}$ percentile** | |
| **Biomass burning** | **23.1** | 21.1 - 24.8 | | **14.3** | 13.2 – 16.0 | | **10.6** | 9.9 – 11.7 | | **6.4** | 6.0 – 7.3 | |
| **Fossil fuel** | **13.7** | 12.7 – 14.2 | | **10.2** | 9.6 – 10.4 | | **8.8** | 8.2-9.1 | | **8.6** | 7.6-8.9 | |

Table S2 $b_{ap}$-to-EC ratios for biomass burning and fossil fuel emission sources as measured in atmosphere and assessed by the multi-time model. Values measured in atmosphere ($b_{ap}$/EC, $\sigma$ and $R^2$) result from a linear regression between experimental $b_{ap}$ and EC concentrations. Results from multi-time model are retrieved considering the $b_{ap}$ and EC apportioned in each source; the $25^{th}$ and $75^{th}$ percentile is estimated by the bootstrap analysis.